Conical emission of high-power femtosecond laser pulse in the atmosphere

I.S. Golubtsov, V.P. Kandidov, and O.G. Kosareva

M.V. Lomonosov Moscow State University

Received April 18, 2001

The most complete (among the earlier considered) model of nonstationary nonlinear optical interaction of high-power femtosecond pulsed laser radiation with air medium is proposed. Taking into account the delay of the Kerr response of the medium, contribution of the material dispersion in the third-order approximation, and application of the Perelomov–Popov–Terent'ev model of photoionization adequate to the experimental data allowed us to obtain results, which well agree quantitatively with the experiment. It is shown that the conical emission of supercontinuum results from the pulse self-phase modulation in space and time under the conditions of strong optical nonlinearity of a highly localized light field.

Introduction

Superbroadening of a high-intensity laser pulse spectrum in air repeatedly attracts the attention of investigators. This effect[1] was discovered in the 70s, when studying the process of high-power laser pulse propagation through condensed media and gases at high pressure. With femtosecond laser pulses, this effect can be observed under natural atmospheric conditions.[2]

High-power femtosecond laser pulses propagating in air give rise to filamentation, at which the large part of the pulse energy is localized in a narrow near-axis zone about 100 μm in diameter and more than 100 m in length. In the first experiments on filamentation,[3–6] subpicosecond titanium-sapphire laser pulses with the peak power of 5–50 GW were used. Then filamentation of the pulsed radiation was obtained at the wavelength of 1.053 μm (Ref. 7) and in the near UV region at the wavelength of 248 nm (Ref. 8).

Filamentation is accompanied by generation of conical emission – supercontinuum – that propagates forward in a narrow cone with the divergence of 2–3° enveloping the filament.[3,4,9] The pulse of the supercontinuum conical radiation is now considered as a promising source for laser sensing and monitoring of the atmosphere. The first lidar experiments with such sensing pulses[10,11] were conducted at Friedrich Schiller University of Jena (Germany). They demonstrated a possibility of obtaining high-resolution absorption spectra in a wide spectral range.

At filamentation, the spectrum of a subpicosecond high-power Ti:sapphire laser pulse broadens from the wavelength of 0.76–0.8 to 0.5 μm to the anti-Stokes region (Ref. 9). The recent experiments conducted by German and French research groups have shown that at filamentation of 800 nm radiation (pulse duration of 35 fs, peak power of 2 TW) the supercontinuum is generated,[12] whose frequency band ranges from 300 nm to 4.5 μm. The spectral intensity of the supercontinuum decreases with increase of frequency shift, and at the band boundaries it is 3 to 4 orders of magnitude lower as compared to the intensity at the laser pulse frequency. However, the intensity at this frequency in the filament is as high as 10^{13}–10^{14} W/cm^2, and the supercontinuum is a pulsed broadband source of high spectral brightness.

Such sources open up principally new possibilities to laser sensing of the atmosphere. A pulse of a broadband lidar covers the continuum spectrum of wavelengths from the visible region to the infrared. The received scattering signal bears a large body of information on the state of the atmosphere, which principally cannot be obtained in fixed or tunable multi-frequency lidars. This offers an opportunity to obtain quickly the spectral pattern of the atmosphere and to conduct its real time monitoring. In addition, the controllable frequency selection of the lidar signal in the receiving system allows the needed spectral resolution to be obtained in the spectral region of interest.

Note that the possibility of creating sources for broadband lidars with continuous or discrete spectra in a certain band, for example, based on optical parametric generators, is now under discussion.[13]

A large number of papers are devoted to theoretical and experimental study of the superbroadening mechanism of a laser pulse frequency spectrum; a brief review of the earliest papers can be found in Ref. 1. In many papers, an attention was paid to connection between the process of frequency spectrum broadening and radiation self-focusing. However, the unified pattern of evolution of the spatiotemporal shape and the frequency-angular spectrum of a high-power laser pulse in air was formed from numerous contradictory concepts.

The review by Genshaw and Cantrell (Ref. 14) is one of the first papers considering the conical emission as a result of simultaneous variation of frequency and angular spectra of a laser pulse. It is numerically shown in this paper that in the case of resonance interaction of laser radiation with a two-level atomic medium, space

0235-6880/01/05 303-13 $02.00

and time modulation of the pulse leads to appearance of essentially nonplanar solitary waves, whose spectrum includes side frequencies propagating at some angle to the axis. Therewith, the radiation self-focusing is not a necessary factor for generation of the conical emission, but it favors shifting the power maximum of the conical emission to larger divergence angles due to increase of the spatial gradient of intensity.

The effect of self-focusing on the discrete supercontinuum generation is also discussed in Ref. 15, which studies experimentally the rotational-vibrational Raman scattering and cascade processes at propagation of high-intensity picosecond laser pulses in high-pressure hydrogen. Lines of the quasi-rotational Raman spectrum at the pressure of 100 bar range from the pumping wavelength of 1.06 μm to 0.4 μm. Unfortunately, the authors do not interpret the formation of divergent rings corresponding to the discrete continuum harmonics, observed under conditions of slight focusing of the pumping beam.

To explain the mechanism of appearance of the conical emission and superbroadening of the pulse spectrum, various physical models are used. Many of them involve the hypothesis on self-trapping of a high-power femtosecond laser pulse due to stabilization of Kerr self-focusing as the laser plasma arises in air.[3,4,16] Actually, the intensity growth at high-power laser pulse self-focusing in air is restricted by strong defocusing in the induced laser plasma, the probability of whose generation increases drastically as the intensity at the nonlinear focus becomes equal to the photoionization threshold. For example, for the radiation at the Ti:sapphire laser wavelength, the photoionization threshold in air is 10^{13}–10^{14} W/cm^2, and the concentration of electrons is estimated as 10^{16} cm^{-3} (Refs. 3 and 4).

In spite of the fact that the processes of establishment of nonlinear polarizability in neutral molecules of the air medium and in the induced laser plasma significantly differ, the followers of the hypothesis on self-trapping assume the stabilization of the space and time profile of the pulse and its spectrum. This assumption is based, to a certain degree, on measurements of the energy density distribution in the pulse cross section and its frequency spectrum; see, for example, Ref. 3.

Some papers[17,18] use the model, according to which the conical emission arises at four-wave parametric conversion. In Ref. 17, at focusing of subpicosecond 1-μJ pulses into a thin glycol jet, a ring structure was observed, in which the ring radius increased with the increase of the frequency shift. These results were interpreted as four-photon parametric generation on the surface of the generated filament.

In Ref. 18, based on numerical solution of the nonlinear Schrödinger equation with instantaneous Kerr nonlinearity and the dispersion of the group velocity in air, it was concluded that the divergence of harmonics of the broadened spectrum follows from the phase relationships for four-wave mixing of two pump waves at the basic frequency, the signal wave with the frequency shift and cross component of the wave vector, as well as the corresponding idle wave. However, this model cannot explain the observed asymmetry of the frequency spectrum of the conical emission and the order of its harmonics in the angular spectrum.[19] Besides, not all waves taking part in this conversion were found experimentally.[14]

In the other model,[3,4,19,20] the conical emission is interpreted as Cherenkov radiation on the surface of a filament that is formed under conditions of Kerr self-focusing and defocusing in the self-induced laser plasma. In Ref. 19, the supercontinuum of the ring structure was observed at the 1.06 μm laser pulse focusing in water and heavy water. The divergence angle of the conical emission was independent of the pulse focusing radius. To explain the appearance of such radiation, it was assumed that the velocity of the laser-induced nonlinear polarization spreading in the filament exceeds the phase velocity at continuum frequencies.

In Ref. 19, it was also noticed that the frequency spectrum superbroadening in experiments is usually accompanied by angular divergence of generated harmonics. For the observed regularity, Golub[19] proposed the term *conical emission of supercontinuum*, which well determines the change of the pulse frequency-angular spectrum as a single phenomenon.

In Ref. 21, the concept of indivisible connection between variations of space and time parameters of laser radiation in a nonlinear medium has been theoretically developed. This paper considers numerically the problem of propagation of a focused laser beam in the high-pressure argon. Spectral maps illustrating the distribution of a pulse frequency broadening over its cross section were obtained by solving the equation of quasi-optics with instantaneous Kerr nonlinearity and nonlinearity in self-induced laser plasma. Rae[21] formulated a simple idea, according to which as the blue shift of the spectral components of continuum increases, the angular divergence of these components must increase, because in the nonlinear increment of the refractive index the increase with time of the gradient is connected with the higher spatial gradient.

The appearance of the spatial self-phase modulation of the light field and, as a consequence, radiation divergence at changes of the refractive index of some nonlinear medium in the plane of beam cross section became the main conclusion of Ref. 22. The work was devoted to theoretical and experimental study of picosecond laser pulse propagation in a quasi-resonance medium – cesium and barium vapors.

In Refs. 6, 9, 23, and 24 the model of generation of the conical emission of supercontinuum is successively developed as a result of self-phase modulation of radiation in space and time at propagation of a high-power femtosecond laser pulse in air. According to this model, high space and time localization of the light

field in a high-power laser pulse at strong optical nonlinearity of the air medium results in formation of the dynamic field of the nonlinear phase change with high spatial and temporal gradients.

The phase change in time causes broadening of the frequency spectrum, while its change in the plane normal to the direction of propagation causes broadening of the angular spectrum. Consideration of the dynamic field of phase change intimately connects the contribution of Kerr self-focusing, plasma nonlinearity, wave effects of diffraction, and material dispersion of the air medium to formation of the frequency-angular spectrum of the conical emission of supercontinuum.

For the simple model[6,9] of self-phase modulation, ignoring dispersion and nonstationarity of the Kerr effect in air, the qualitative agreement has been obtained between calculated and experimental data.

In this paper, to describe the process of generation of the conical emission of supercontinuum, a model of nonstationary nonlinear optical interaction of a high-power femtosecond laser pulse with the air medium is proposed. This model is most complete among the earlier models. It includes the contribution of material dispersion in the third-order approximation and nonstationarity of the cubic susceptibility component of neutral air molecules. For the first time, this model uses the Perelomov–Popov–Terent'ev (PPT) photoionization theory[25] to describe the process of generation of femtosecond laser plasma. The equivalent charge of a single-ionized oxygen molecule (fitting parameter of the model) is estimated therewith from the experimental data on photoionization of gases at the atmospheric pressure.[26]

Dynamic model of nonlinear optical interaction of high-power femtosecond laser pulses with the air medium

When passing in air, the high-power laser radiation experiences nonstationary self-action because of the refractive index dependence on the radiation intensity. For subpicosecond laser pulses, this dependence is determined by cubic susceptibility of neutral atoms and molecules of the air medium and nonlinearity of the laser plasma arising due to photoionization in the strong light field of the pulse.

Kerr nonlinearity

Nonlinearity of atoms and molecules is caused by anharmonism of the electron response, as well as Raman scattering involving rotational transitions of molecules of the medium.

The time of establishment of the electron response is about 10^{-15} s, and this mechanism can be thought non-delay for subpicosecond pulses. Therefore, a nonlinear addition to the refractive index Δn_K^e for the electronic Kerr effect is determined as:

$$\Delta n_K^e = (1 - g)\,\frac{1}{2}\,n_2\,|E|^2, \qquad (1)$$

where E is the complex amplitude of the electric field, and the coefficient g is proportional to the ratio of the contribution of the delay mechanism to the nonlinear addition to the refractive index. This coefficient can take the values from 0 to 1.

The contribution to the cubic susceptibility from stimulated Raman scattering involving rotational transitions of anisotropic molecules of air has the characteristic transient period of about 10^{-13} s (Refs. 27–29). Consequently, it has some delay for subpicosecond pulses.

The data on the relation between the delay and non-delay contributions to the cubic susceptibility are the following. In Ref. 30, it is shown, based on the measured nonlinear polarizability of the air, that the contribution of the non-delay electronic mechanism is negligibly small. At the same time, Shimoji et al.[31] measured the contribution of the mechanism of Raman scattering in the absence of other nonlinear effects distorting the true pattern (this was not done in Ref. 30). Analysis of the results of Ref. 31, as well as Ref. 28, suggests that the contributions of the both mechanisms of nonlinear response to the common change of the refractive index of the medium are roughly equal. Thus, $g = 1/2$.

Taking into account the delay of the medium response, the equation for the nonlinear addition Δn_K^R from Raman scattering involving rotational molecular transitions has the form[32]:

$$\Delta n_K^R(r, t) = g \int_{-\infty}^{t} \frac{1}{2}\,n_2\,|E(r, t')|^2 H(t - t')\,dt'. \qquad (2)$$

The function of response $H(t)$ describes the process of establishment of inertial nonlinearity. In Refs. 27 and 28 it was shown to have a complex oscillating character. In Ref. 32, the response function $H(t)$ measured in Ref. 28 is approximated based on the damped oscillator model by the following equation:

$$H(t) = \theta(t)\,\Omega^2 \exp\left(-\frac{\Gamma t}{2}\right)\frac{\sin(\Lambda t)}{\Lambda}, \qquad (3)$$

where $\theta(t)$ is the Heaviside function, and $\Lambda = \sqrt{\Omega^2 - \Gamma^2/4}$.

The fitting parameters have the following values: $\Omega = 20.6$ THz and $\Gamma = 26$ THz. From the form of the response function we can conclude that two characteristic periods are present in the process of establishment of the nonlinear response: the delay τ_1 and the period of oscillations of the response function τ_2; these parameters can be expressed through the fitting parameters Γ and Λ determined in Ref. 32:

$$\tau_1 = \frac{2}{\Gamma}, \quad \tau_2 = \frac{1}{\Lambda}. \qquad (4)$$

Thus, the characteristic periods are $\tau_1 = 77$ fs and $\tau_2 = 160$ fs. These values are comparable with the laser pulse duration in the laboratory experiment on observation of the conical emission.[3–5] Therefore, the allowance for the delay of the nonlinear contribution of scattering to variations of the refractive index Δn_K^R is important for adequate description of the process of the pulse self-action.

Plasma nonlinearity

Laser plasma arises due to multi-photon and tunnel ionization of molecules of air under exposure to high-power laser radiation. Formation of the plasma leads to the change of the refractive index Δn_p, which is described as follows:

$$\Delta n_p = -\frac{2\pi e^2 N_e}{m(\omega^2 + \nu_c^2)}\left(1 - i\frac{\nu_c}{\omega}\right), \qquad (5)$$

where ω is the central frequency of the pulse spectrum; m and e are the electron mass and charge; N_e is the concentration of free electrons; ν_c is the effective frequency of electron collisions with gas molecules.

In Ref. 33, the value of ν_c in air was estimated. According to this estimate, the effective frequency of collisions ν_c is small as compared to the radiation frequency ω characteristic of the experiments described in Refs. 3–5 and 9. This allows Eq. (5) to be rewritten in the following approximate form:

$$\Delta n_p = -2\pi e^2 N_e/(m\omega^2)\,. \qquad (6)$$

The concentration of free electrons N_e in the approximation of single ionization at every point in space and time is determined by the rate equation

$$\frac{\partial N_e}{\partial t} = R(I)\,(N_0 - N_e), \qquad (7)$$

where N_0 is the concentration of neutral air molecules before ionization. The designation $R(I)$ is used for the rate of ionization of the oxygen molecule, whose ionization potential is 12.1 eV. Photoionization of other air constituents can be neglected. Actually, the ionization potential of the nitrogen molecule is equal to 15.6 eV, and the threshold of multi-photon ionization at the wavelength of the Ti:sapphire laser turned to be much higher than that for oxygen. The total concentration of molecules of other gaseous constituents does not exceed 1%, and they can be neglected.

For calculating the ionization rate of the oxygen molecule $R(I)$, the PPT model is applied; this model describes the process of ionization of hydrogen-like atoms. In accordance with Ref. 25, the total rate of ionization of an atom by a plane polarized wave from the state with quantum numbers l and m is the following:

$$R = |C_{n^*l^*}|^2 f_{lm} E_i \sqrt{\frac{6}{\pi}}\left(\frac{2(2E_i)^{3/2}}{F}\right)^{2n^* - |m| - 3/2} \times$$

$$\times (1+\gamma^2)^{|m|/2+3/4} A_m(\omega,\gamma)\; e^{-\frac{2(2E_i)^{3/2}}{3F}g(\gamma)}, \qquad (8)$$

where $\gamma = \omega\sqrt{2E_i}/F$ is the Keldysh adiabatic parameter; E_i is the ionization potential of the atom; F is the amplitude of the laser electric field; $n^* = Z/\sqrt{2E_i}$, and $l^* \approx n^* - 1$. The coefficients entering into Eq. (8) are determined as:

$$f_{lm} = \frac{(2l+1)\,(1+|m|)!}{2^{|m|}\,|m|!(1-|m|)!}\,,$$

$$g(\gamma) = \frac{3}{2\gamma}\left[\left(1+\frac{1}{\gamma^2}\right)\mathrm{Arsh}(\gamma) - \frac{\sqrt{1+\gamma^2}}{2\gamma}\right],$$

$$|C_{n^*l^*}|^2 = \frac{2^{2n^*}}{n^*\Gamma(n^*+l^*+l)\,\Gamma(n^*+l^*)}\,,$$

$$A_m(\omega,\gamma) =$$

$$= \frac{4\gamma^2}{\sqrt{3\pi}|m|!(1+\gamma^2)}\sum_{n>\nu}^{\infty} w_m\left(\sqrt{\frac{2\gamma(n-\nu)}{\sqrt{1+\gamma^2}}}\right) e^{-(n-\nu)\alpha(\gamma)},$$

where

$$w_m(x) \equiv e^{-x^2}\int_0^x (x^2 - y^2)^{|m|}\, e^{y^2}\, dy,$$

$$\alpha(\gamma) \equiv 2\left(\mathrm{Arsh}(\gamma) - \frac{\gamma}{\sqrt{1+\gamma^2}}\right);\quad \nu \equiv \frac{E_i}{\omega}\left(1+\frac{1}{2\gamma^2}\right).$$

When calculating $R(I)$, only single ionization of the atom was taken into account, because the probabilities of double and multiple ionization are small as compared to the probability of single ionization. In accordance with the theory described in Ref. 25, the effective charge of a single-ionized atom is equal to unity. However, in this work the effective charge was taken equal to 0.5, which value is in close agreement with the experimental results on ionization of molecular oxygen.[26]

Material dispersion

The operating wavelength of the Ti:sapphire laser ($\lambda = 0.76 - 0.80$ μm) is far away from absorption lines of atmospheric gaseous constituents. Therefore, the approximated dispersion theory can be used to describe the material dispersion of air. According to Ref. 34, the dispersion length for the 230-fs-long laser pulse at the wavelength of 800 nm is longer than 1 km; this value far exceeds the length of the observed filaments. However, as the pulse propagates under the Kerr nonlinearity conditions, the leading front of the pulse sharpens and 10–20-fs-long spikes appear. For such a time scale of the light field variation, the dispersion

length shortens down to several meters; this value is already comparable with the characteristic length of a filament in the experiments.[3–5,9] Therefore, the dispersion in air should be necessarily taken into account.

The theoretical calculations[28,32] are usually restricted to the terms of the second order of the dispersion theory. In Ref. 34, it was shown that the dispersion of the group velocity significantly restricts and slows down the intensity growth at the leading front of the pulse at Kerr self-focusing. Simultaneously, the pulse decays into a series of spikes. Such transformation of the field distribution in space and time leads to the change in the frequency-angular spectrum of the pulse. According to Ref. 24, short-wave components propagating at an angle to the optical axis arise in the pulse spectrum; just these components form the conical emission.

However, as the small-scale time structure is formed in the pulse, the contribution of the higher-order terms of the series in the dispersion theory may be significant. In this paper, the material dispersion of neutral air constituents was considered in the third-order approximation of the dispersion theory. To calculate the derivatives k'_ω, k''_ω, and k'''_ω of the wave number k, the Cauchy equation for the air under standard conditions (T = 293 K, P = 101325 Pa) was used[35]

$$n(\lambda) = \left(2726.43 + \frac{12.29 \cdot 10^6 \text{ nm}^2}{\lambda^2}\right) \cdot 10^{-7} + 1. \quad (9)$$

Under such conditions, the coefficients of expansion of the wave number into the Taylor series in terms of the frequency in the vicinity of the laser frequency take the following values: $k'_\omega = 3.3 \cdot 10^{-9}$ s/m, $k''_\omega = 1.6 \cdot 10^{-29}$ s^2/m, $k'''_\omega = 6.9 \cdot 10^{-45}$ s^3/m.

Mathematical model

The smallest time scale of field variation is several tens of femtoseconds, and the method of slowly varying amplitudes is applicable to the problem of pulse propagation. In this approximation, the equation for the light field amplitude has the form

$$2ik\left(\frac{\partial}{\partial z} + \frac{1}{v_g}\frac{\partial}{\partial t}\right)E = \Delta_\perp E - k\, k''_\omega \frac{\partial^2 E}{\partial t^2} +$$

$$+ i\left(k'_\omega k''_\omega + \frac{1}{3}k\, k'''_\omega\right)\frac{\partial^3 E}{\partial t^3} + \frac{2k^2}{n_0}\Delta n E - ik\alpha E, \quad (10)$$

where v_g is the group velocity of the pulse.

The first term in the right-hand side describes beam diffraction; the second and the third terms correspond, respectively, to beam dispersion in the second and the third approximations of the dispersion theory; the fourth term describes the refractive index variation due to Kerr and plasma nonlinearities, and, finally, the fifth term describes the pulse energy absorption at ionization of the medium.

The nonlinear addition to the medium refractive index consists of two terms corresponding to the contributions from Kerr and plasma nonlinearities: $\Delta n = \Delta n_K + \Delta n_p$. The dependence of Δn_K on the intensity I is determined by the equation following from Eqs. (1) and (2):

$$\Delta n_K = (1 - g)\frac{1}{2} n_2 |E|^2 + g\int_{-\infty}^{t} \frac{1}{2} n_2 |E(r, t')|^2 H(t - t')\mathrm{d}t', \quad (11)$$

where the first term equals the instantaneous contribution from the electronic Kerr effect, and the second term equals the contribution due to stimulated Raman scattering involving rotational transitions of air molecules.

The coefficient $\alpha = I^{-1} l\hbar\omega(\partial N_e/\partial t)$ reflects energy absorption at ionization of the medium, where $I = (cn_0/8\pi)|E|^2$ is the intensity of the electric field; l is the number of photons involved in the process (l is 7.4–7.8 for λ = 0.76–0.80 μm).

Thus, equations (3), (6)–(8), (10), and (11) form a closed system describing the evolution of a laser pulse in space and time and, consequently, variation of the pulse frequency-angular spectrum as the pulse propagates in air.

The initial space and time distribution of the field of the input pulse was set in the following form:

$$E(r, z = 0, \tau) = E_0 \exp\left[-\frac{r^2}{2a^2} - \frac{\tau^2}{2\tau_0^2}\right], \quad (12)$$

where $\tau = t - z/v_g$ is the time in the moving coordinate system; $2\tau_0$ is the pulse duration, and a is the beam radius.

Numerical scheme

Passing to the dimensionless variables in Eq. (10)

$$z' = \frac{z}{L_{dif}}, \quad t' = \frac{\tau}{\tau_0} = \frac{t - z/v_g}{\tau_0}, \quad r' = \frac{r}{a},$$

$$E' = \frac{E}{E_0}, \quad I' = \frac{I}{I_0}$$

and omitting the primes, we derive the following equation:

$$2i\frac{\partial E}{\partial z} = \Delta_\perp E - \frac{L_{dif}}{L^{(2)}_{disp}}\frac{\partial^2 E}{\partial t^2} + i\frac{2}{3}\frac{L_{dif}}{L^{(3)}_{disp}}\frac{\partial^3 E}{\partial t^3} +$$

$$+ \left(\frac{2k}{n_0}\Delta n E - i\alpha E\right)L_{dif}, \quad (13)$$

where $L^{(2)}_{disp} = \dfrac{\tau_0^2}{|k''|}$, $L^{(3)}_{disp} = \dfrac{2\tau_0^3 k}{|kk''' + 3k'k''|}$, $L_{dif} = ka^2$ are the dispersion lengths in the second and third approximations of the dispersion theory and the

diffraction length, respectively. The variable $r = \sqrt{x^2 + y^2}$ is used because of the axial symmetry of the problem.

In numerical simulation of the parabolic equation, the method of splitting into physical factors is applied. The diffraction equation is solved by the absolutely stable Crank–Nicholson scheme with the use of the sweep method. The dispersion equation, in the spectral representation, is calculated separately for every harmonic. The fast Fourier transform method is used for transition into the spectral domain.

The dimensions of the domains along the coordinates r, z, and t in numerical simulations were $6a$, L_{dif}, and $10\tau_0$, respectively. The number of nodes falling on these domains were taken to be 1024, 8614, and 512. This provided for adequate description of the imaginary and real parts of the complex field amplitude.

Parameters of the task

To study the mechanism of generation of the conical emission of supercontinuum based on the set of equations (3), (6)–(8), (10), and (11), a laser pulse with the parameters corresponding to the laboratory experiment[5] was considered. As a result, the quantitative wavelength dependence of the radiation angular divergence has been obtained.

With the initial space and time distribution of the light field in the form (12), the pulse duration parameter is $\tau_0 = 138$ fs. This value corresponds to the full duration of 230 fs at the intensity distribution halfwidth. The values of the peak radiation intensity and the beam radius were chosen close to the corresponding values at the beginning of filamentation: $I_0 = 10^{13}$ W/cm^2 and $a = 167$ μm. This choice is determined by limited capabilities of numerical analysis. Numerically, it is still impossible to reconstruct simultaneously the field variations of the initial pulse with the parameters, corresponding, e.g., to the experiment described in Ref. 5 ($I_0^{\text{exp}} = 10^{11}$ W/cm^2, $a^{\text{exp}} = 3.5$ mm), and the filament pulse, whose fine structure has the scale of the order of tens of micrometers and the peak intensity takes the values $I_0 = 10^{13}$–10^{14} W/cm^2. Under conditions of the experiment from Ref. 5, the characteristic scales of the field variation along filament, the diffraction length and dispersion length are: $L_{\text{dif}}^{\text{exp}} = 96$ m and $L_{\text{disp}}^{(2)/\text{exp}} = 1200$ m.

Evolution of the space and time shape of the pulse

The amplitude-phase radiation conversion caused by the nonlinear response of neutral atoms and molecules of the air medium, as well as the induced laser plasma, as well as the effects of dispersion and diffraction lead to the complex dynamic redistribution of the power in the beam cross section. Figure 1 shows transformation of the pulse shape at filamentation.

It is seen that at the distances less than 20 m the process of propagation is largely affected by self-focusing. As a result, the beam energy is concentrated near the beam axis. At long distances ($z = 35$ m), as the peak intensity achieves 10^{14} W/cm^2, the electron concentration increases sharply, what results in defocusing of the pulse trailing edge and appearance of a system of aberration rings in the power density distribution.

Analysis of these results in comparison with the results obtained earlier for a simpler model[34] indicates significant influence of the Kerr response delay and the third-order material dispersion of the air medium on the pulse evolution. The delay of the nonlinear response causes the time redistribution of the power density. This manifests itself in smoothing of the generated intensity spikes and decrease of their contrast. The peak intensity in the filament decreases by 1.5–2 times. At long distances, e.g., $z > 50$ m, the spiking structure characteristic of the model with instantaneous Kerr nonlinearity is partially suppressed.[34] As this takes place, the intensity of the remains of spikes increases.

This pattern reflects formation of the dynamic ring structure in the cross-section intensity distribution in the filamentation zone (Fig. 2). Kerr self-focusing causes formation of an intensity peak at the leading edge of the pulse (at $t = -0.38\tau_0$). The peak is then replaced by a system of concentric rings at the pulse center and at the trailing edge (at $t = 0.38\tau_0$).

Formation of ring intensity peaks in the filament can be qualitatively explained in the following way. The wave divergent from the axis due to defocusing in the induced laser plasma interferes with the wave convergent to the center due to the influence of Kerr focusing at the beam periphery, where the intensity is still insufficient for photoionization.

The energy density distribution in the cross section of a femtosecond laser pulse was recorded experimentally. The energy density, as a result of integration of the time distribution of intensity during the pulse, has a smoother ring structure (Fig. 3). The energy rings exist only in the zone of developed filamentation, where the ring peaks in the intensity distribution are high enough.

Observation of the ring structure in the distribution of the energy density has been reported in Ref. 36, which considered focused beams. In that experiment, a wave from the beam periphery converges due to not only Kerr nonlinearity, but also initial focusing of radiation. As a result, the angle, at which the interfering waves converge, increases, and a system of closely separated interference fringes is observed.

Figure 4 demonstrates the variation with the distance z of radial distribution of the energy density in the filament. The maximum value of the density at the filament axis varies nonmonotonically along its length.

Sharp growth of the energy density at the beginning of the filament is followed by its decrease because of formation of divergent rings at plasma defocusing. The repeated increase of the energy density at $z = 50$ m is caused by contraction of intensity rings to the axis because of the focusing curvature of the wave front at the beam periphery at Kerr focusing. In Fig. 1, the process of ring contraction manifests itself in formation of the intensity spike on the axis for $t = 2\tau_0$ at $z > 50$ m. This mechanism qualitatively explains the effect of re-focusing observed in Ref. 5 and confirmed by numerical experiments.[5,32]

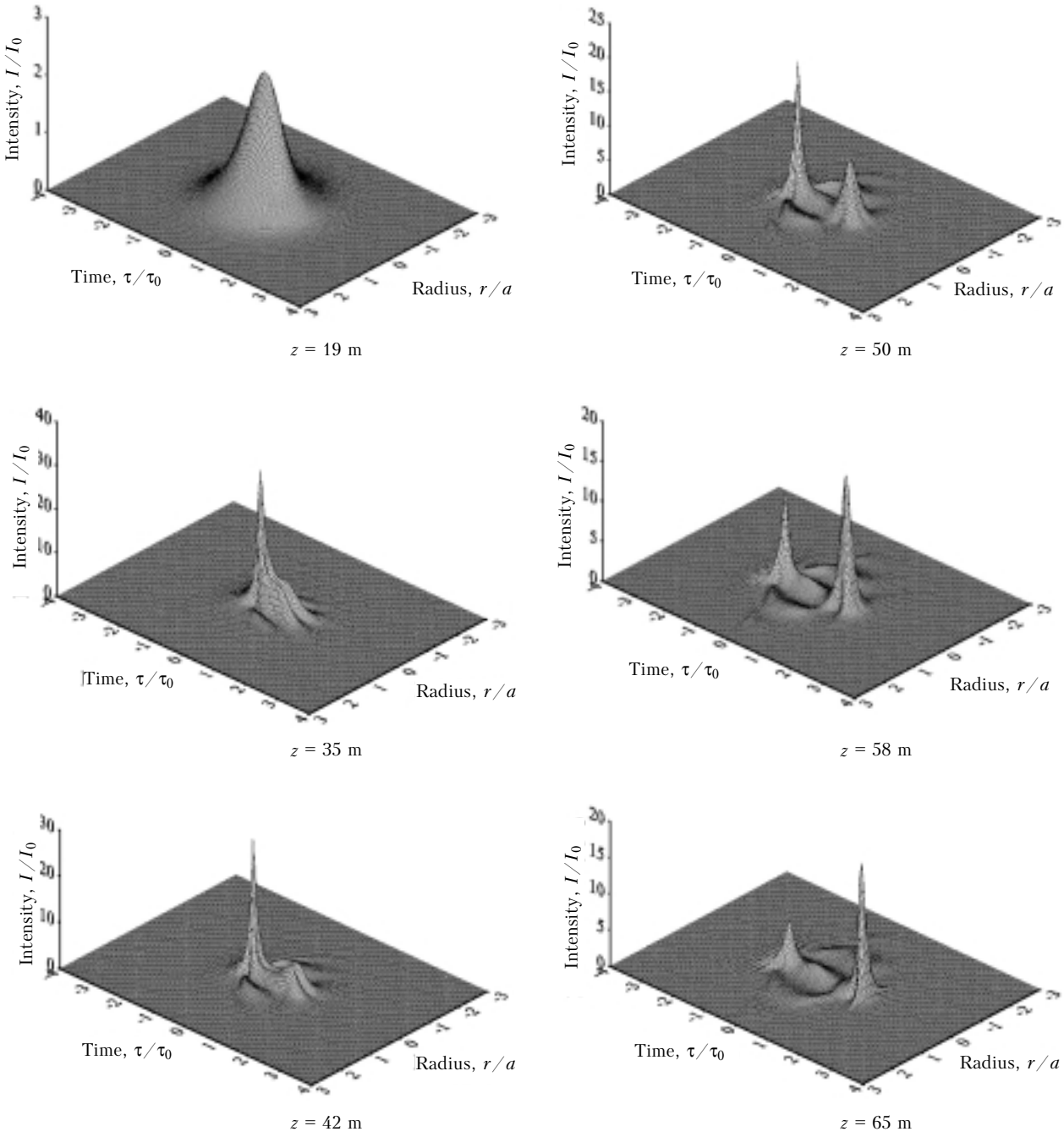

Fig. 1. Evolution of the intensity I in the pulse with the peak power $P_0 = 9$ GW ($P_0 = 5P_{\text{th}}^{\text{teor}}$), the duration parameter $\tau_0 = 138$ fs, the normalized radius corresponding to $a = 3.5$ mm. The intensity I is normalized to $I_0 = 10^{13}$ W/cm^2.

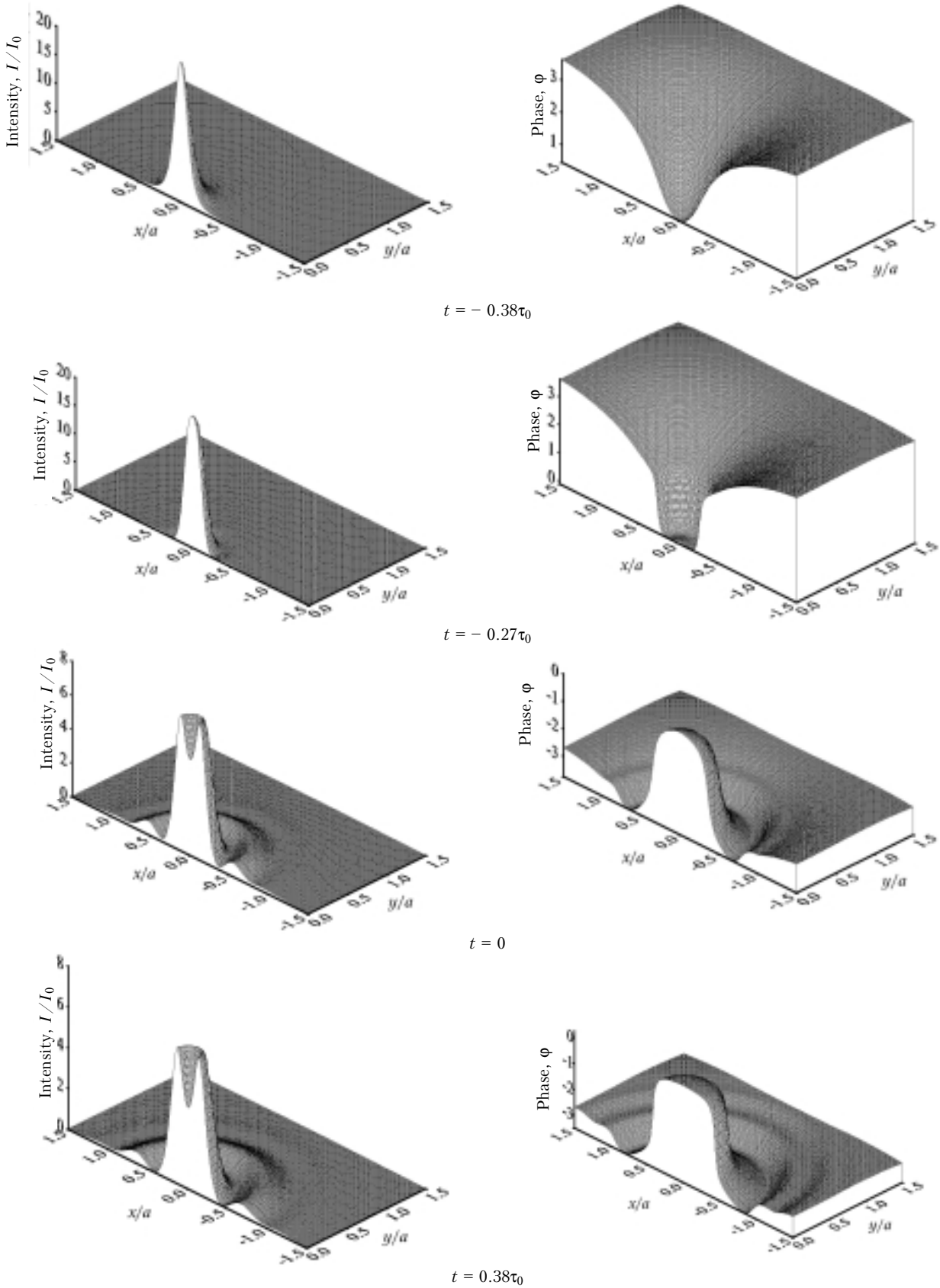

Fig. 2. Spatial distribution of intensity I (left) and phase φ (right) in the plane transverse to the propagation direction at different time moments. The intensity I is measured in the units of I_0; the phase is given in radians; the distance $z = 35$ m.

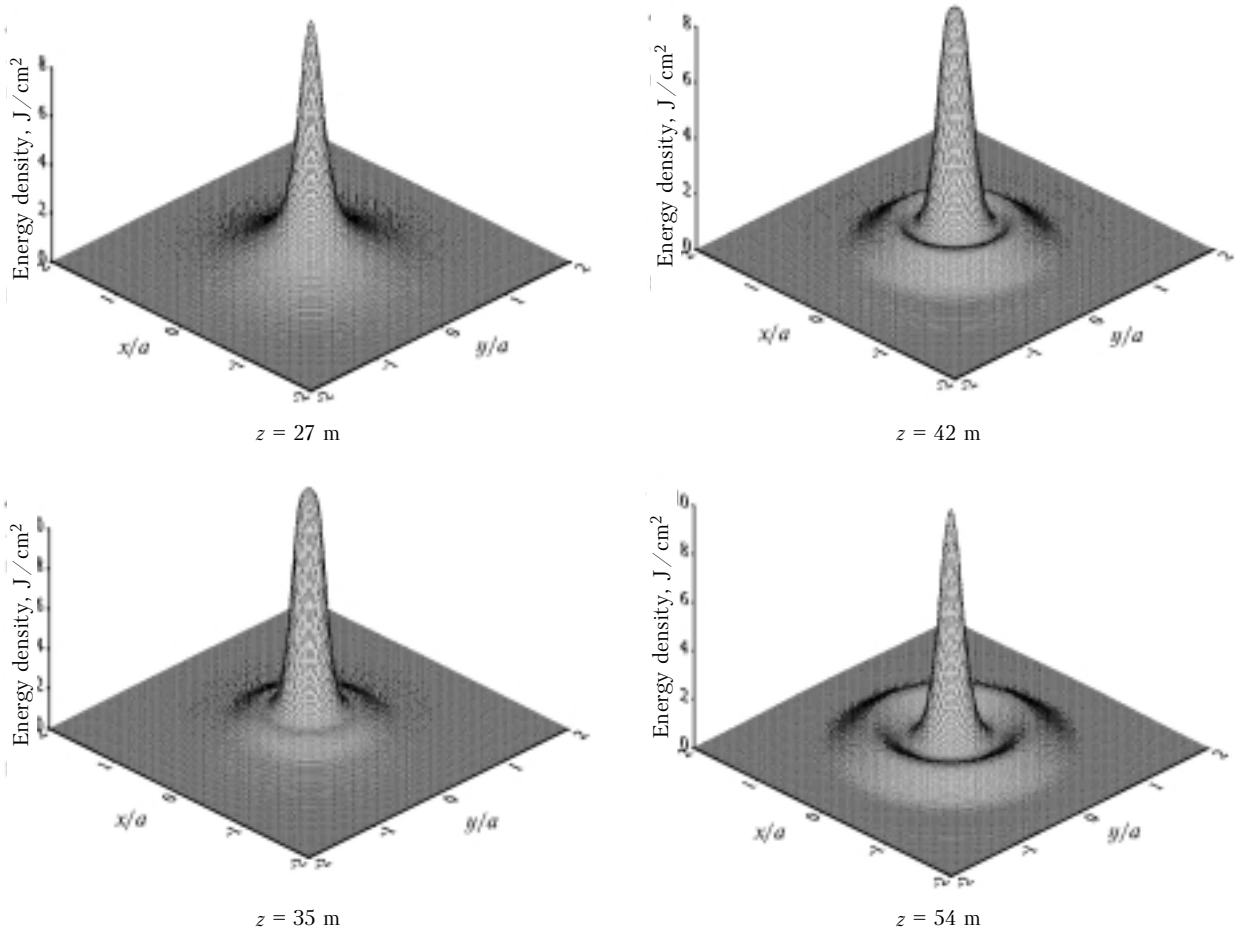

Fig. 3. Variation of the energy density distribution in the pulse cross section as a function of the distance z; a = 3.5 mm.

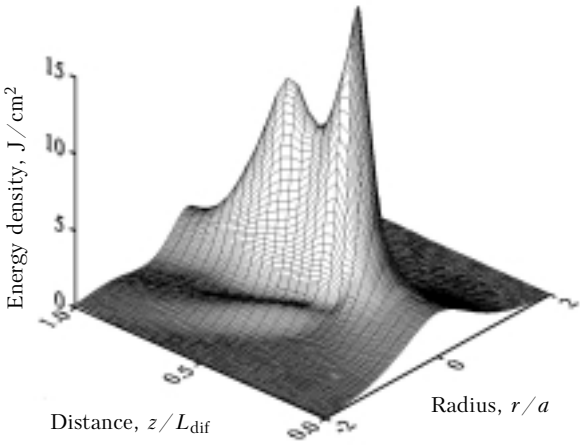

Fig. 4. Radial distribution of the energy density of laser pulse as a function of the distance z. Parameters L_{dif} = 96 m and a = 3.5 mm.

Wave front transformation

The amplitude-phase conversion of radiation caused by nonlinearity and the phase-amplitude conversion caused by diffraction and dispersion join spatially and temporally the evolution of the pulse shape and transformation of the phase φ distribution of the light field. Figure 2 (right) shows the wave front of the light wave at the pulse leading edge at $t = -0.38\tau_0$ and $t = -0.27\tau_0$, at the center at $t = 0$, and at the trailing edge at $t = 0.38\tau_0$ for z = 35 m. In the pulse layer at $t = -0.38\tau_0$, the phase in the near-axis part of the beam ($r < 0.3a$) is delayed because of the Kerr nonlinearity. The local maximum on the axis in the phase distribution at $t = -0.27\tau_0$ indicates that plasma defocusing begins within the narrow near-axis zone, where the intensity achieves the photoionization threshold. For $t = -0.27\tau_0$ plasma defocusing on the axis at the distance of 35 m still does not cause marked redistribution of intensity at the pulse leading edge.

However, by the time layer $t = 0.38\tau_0$, the nonlinear phase change is accumulated at the pulse trailing edge, and the wave front looks like a system of concentric rings. In the zones of intensity localization in ring maxima ($r \approx 0.7a$), the radial gradient of the phase change is positive, thus indicating that intensity rings scatter from the axis in the considered layer at the distance z (see Fig. 1 at z = 35 m).

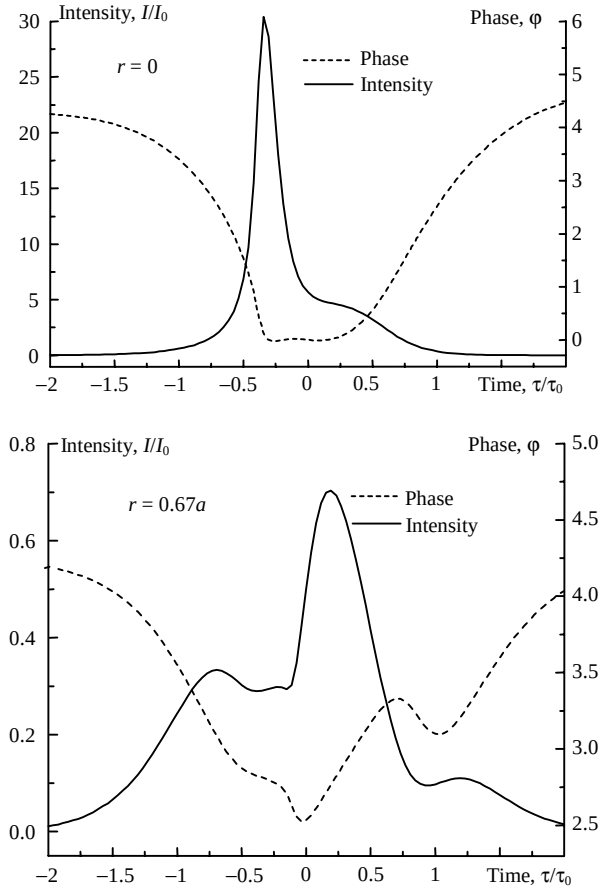

Fig. 5. Evolution of the intensity I (solid curve) and the nonlinear change of the phase φ (dashed curve) on $r = 0$ and off $r = 0.67a$ the axis at the distance $z = 35$ m. The intensity I is measured in units of I_0, and the phase φ is measured in radians.

The ring maximum of intensity in the near-axis zone of the layer is enveloped by a dark ring, in which the intensity is zero. This leads to formation of a phase dislocation at the trailing edge of the pulse at $t = 0.38\tau_0$. The dislocation looks like a ring with the radius $r \approx 0.4a$, at which the field phase jump is equal to π.

Formation of the wave front having a ring structure with the positive radial phase gradient is equivalent to appearance of the transverse component of the wave vector and, consequently, to the generation of the conical emission. To reveal the mechanism of the frequency spectrum broadening, we consider the phase evolution of the light wave in the pulse at the same distance $z = 35$ m (Fig. 5).

The wave phase first decreases because of the positive increment of the refractive index due to the Kerr nonlinearity and then increases due to the negative contribution from the plasma formed after the intensity has achieved the ionization threshold. The decrease of the phase in time leads to the long-wave shift of the radiation, while the phase increase causes the short-wave frequency shift. As this takes place, the intensity spike on the filament axis ($r = 0$) corresponds to the phase minimum, and the frequency shift is symmetric with respect to the frequency. In the off-axis zone ($r = 0.67a$), the intensity peak corresponds to the positive temporal gradient of the phase change. Such character of the self-phase modulation is responsible for generation of the short-wave region of supercontinuum.

Thus, generation of the conical emission of supercontinuum is caused by the self-phase modulation of a laser pulse under the effect of the plasma nonlinearity at high space and time localization of the light field due to Kerr self-focusing of the pulse.

Conical emission of supercontinuum

To analyze quantitatively the nonlinear enrichment of the pulse spectrum, we will calculate the frequency-angular spectrum $U(\theta_x, \theta_y, \Delta\omega, z)$ of the pulse in accordance with the following equation:

$$U(\theta_x, \theta_y, \Delta\omega, z) =$$

$$= \int dx dy\, e^{-i\theta_x kx}\, e^{-i\theta_y kx} \int dt\, e^{-i\Delta\omega t} E(\sqrt{x^2 + y^2}, t, z), \quad (14)$$

where θ_x and θ_y are the angular components of the spatial spectrum and $\Delta\omega$ is the frequency shift of the spectral component. In calculations, we pass from the cylindrical coordinates to the Cartesian ones. Because of the axial symmetry of the initial complex amplitude $E(r, t)$, the angular divergence of θ_x and θ_y along the axes x and y is the same for every component of the frequency spectrum.

Figure 6 shows, in the semi-logarithmic scale, the angular distributions of the intensity for the components of the frequency spectrum $S(\theta, \lambda) = |U(\theta, \lambda)|^2$ at two distances z.

It is seen that harmonics at the wavelengths less than 800 nm are characterized by two maxima diverging symmetrically from the axis. This corresponds to formation of the conical emission. The angular position of the maxima is almost independent of the distance z. It is significant that as the wavelength of the spectral components decreases, their divergence angle in the conical emission increases. At the same time, the maximum of the radiation intensity at the wavelength of 800 nm (main spectral component of the laser pulse) passes along the filament axis.

The full pattern of variation of the pulse frequency-angular spectrum at filamentation is shown in Fig. 7. This figure shows, in the semi-logarithmic scale, the normalized intensity of the spectral components $S(\theta, \lambda)$ depending on their wavelength and the divergence angle.

It is seen that the initially Gauss spectrum experiences serious transformation in the process of filamentation. At the distance $z = 31$ m, the angular divergence of the component at the laser wavelength increases due to the decrease of the cross dimensions of the pulse layers because of self-focusing.

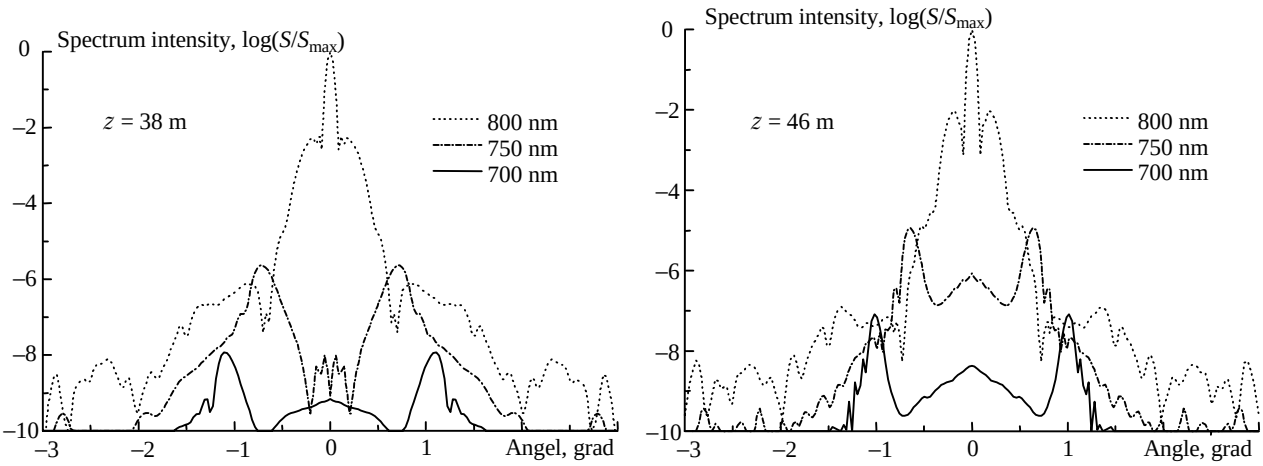

Fig. 6. Angular distributions of frequency spectrum components at different wavelengths for two distances z.

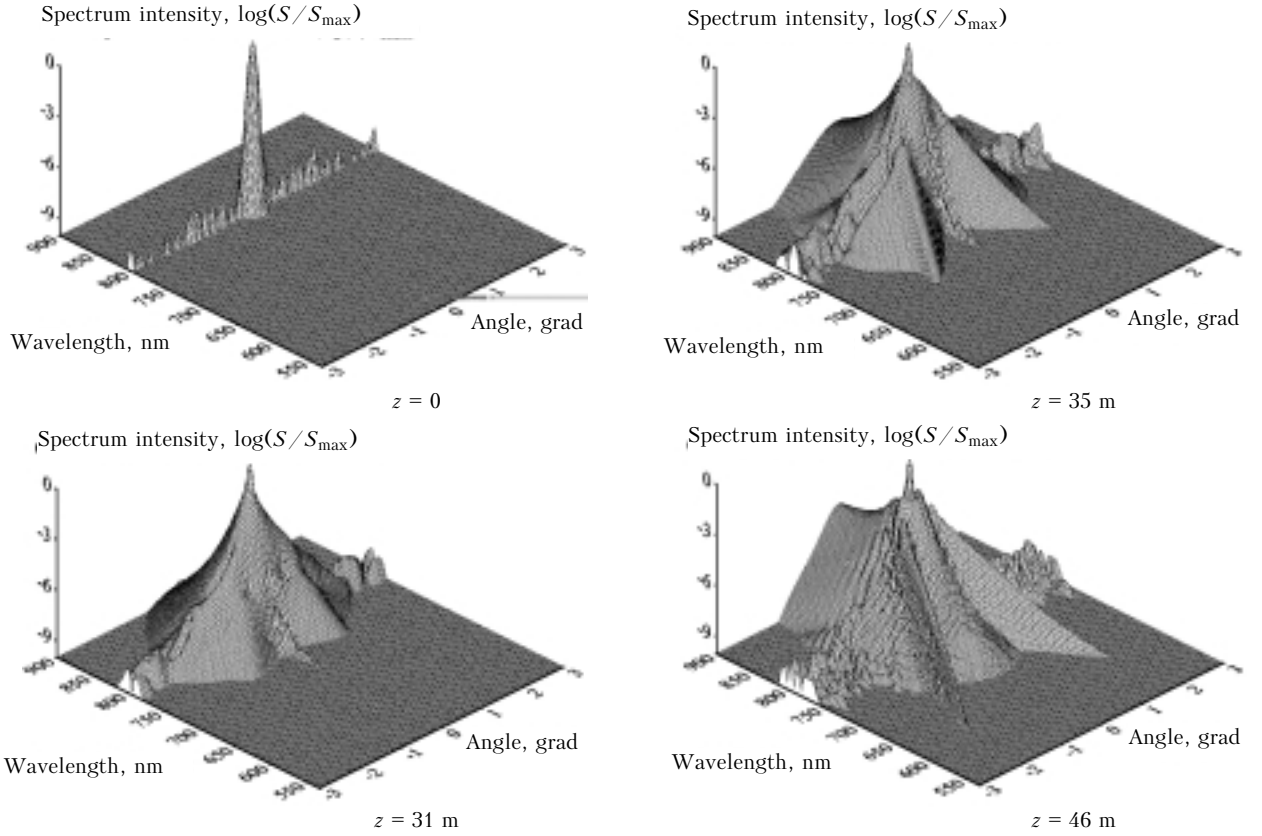

Fig. 7. Evolution of the frequency-angular spectrum of the pulse with the distance z.

However, already at $z = 35$ m the components shifted to the short-wave region become significant in the spectrum. As a result, the supercontinuum is formed ranging from the laser wavelength to 650 nm. The divergence angle of the spectral components increases with the decrease of their wavelength. In Fig. 7, this process is shown as a long drop-down comb corresponding to the conical emission of the short-wave supercontinuum radiation. The comb cross section at $\lambda = \text{const}$ is a single ring of the conical emission.

Role of various factors in formation of conical emission

The experimental data on the angular divergence of conical emission[9] allow us to estimate the adequacy of the model of nonlinear optical interaction of femtosecond laser pulses with the air medium. To estimate contributions of different factors, we consider the wavelength dependence of the divergence angle for

the spectral components of the supercontinuum given by different models (Fig. 8).

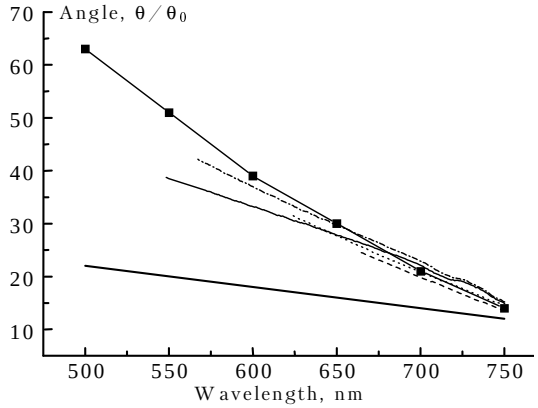

Fig. 8. Wavelength dependence of the divergence angle θ of the conical emission of the supercontinuum. The angle is normalized to the initial beam divergence $\theta_0 = \lambda_0/(2\pi a)$: experiment from Ref. 9 (— —); $Z_{ef} = 0.5$ (·····); the model with delay, $Z_{ef} = 0.72$ (----); third order of the dispersion theory (—·—); second order of the dispersion theory[24] (——); simple model[2,9] (——).

As compared with the results of Refs. 2 and 9, the allowance for the group velocity in the mathematical model of dispersion made much better the quantitative agreement between the experimental and calculated frequency-angular dependences of the conical emission.

Physically, this is explained by the fact that the dispersion effect causes the decrease of the pulse temporal sharpening. As a consequence, the temporal gradient of the light field phase in the induced plasma decreases. As a result, the frequency shift at the dispersion of the group velocity is formed at larger angular shift than in the absence of dispersion. Simultaneously, the maximum value of the short-wave frequency shift decreases.

Based on the above-said, it could be expected that the third-order dispersion would also affect the divergence angle of the conical emission. From Fig. 8 it is seen that as the mathematical models account for the third-order dispersion, the calculated data become closer to the experimental results. The third-order dispersion imparts higher angular divergence to the conical emission. As the wavelength decreases, this effect becomes more significant. On the other hand, broadening of the spectrum to the high-frequency region decreases. This is connected with the fact that distortions of the pulse time shape due to third-order dispersion lead to decrease of the temporal gradients of intensity and electron concentration.

The allowance for the delay of the Kerr nonlinearity in the mathematical model has significantly affected the space and time profiles of the pulse intensity. The logical consequence of this result is the change of the frequency-angular dependence of the conical emission as well. It is seen from Fig. 8 that the conical emission in the medium with delayed Kerr nonlinearity is much weaker, as indicated by the maximum value of the short-wave shift (120 nm). This is connected with the fact that the plasma nonlinearity at the pulse trailing edge is compensated by the delayed contribution of the Kerr nonlinearity from the most intense part of the pulse. The phase gradients decrease, and, consequently, the spectrum width and the angular divergence of the conical emission decrease. It should be noted that in the wavelength region from 680 to 800 nm this model demonstrates a good quantitative agreement between the calculated results and the experimental data.

The results considered above have been obtained for the ionization model with the effective charge of a single-ionized molecule $Z_{ef} = 0.72$. At the same time, in Ref. 26 it was shown that the value $Z_{ef} = 0.5$ gives the best quantitative agreement with the experimental results on ionization of the oxygen molecule.

Figure 8 shows the frequency-angular dependence of the conical emission with allowance made for the delay of the Kerr response, third-order dispersion, and the effective charge $Z_{ef} = 0.5$. Due to application of this ionization model with such a charge the calculated results became closer to the experimental data. The decrease of the effective charge increases the ionization threshold. Consequently, the steepness of the pulse leading edge increases, and free electrons are generated more efficiently. As a consequence, temporal gradients of the phase take large values, thus increasing the short-wave frequency shift of the radiation.

So, the most complete model of nonlinear optical interaction of the radiation with the air medium includes the delay of the cubic susceptibility, third order of the dispersion theory, and more accurate model of photoionization; it demonstrates a good quantitative agreement between the calculated results and the experimental data.

Different physical factors often have opposing effects on the frequency-angular dependence of the conical emission, what underlines the need to take all these factors into account in the model of nonlinear optical interaction of a high-power femtosecond laser pulse with the air medium.

Conclusion

1. Evolution of the space and time shape and the frequency-angular spectrum of a high-power femtosecond laser pulse in air is caused by the nonstationary nonlinear optical interaction of the light field with the gaseous constituents of the air medium and the induced laser plasma, as well as wave effects of dispersion and diffraction. For adequate description of the evolution, numerous factors determining the amplitude-phase conversion of the laser radiation due to optical nonlinearity and the phase amplitude conversion due to wave effects should be carefully taken into account.

2. The proposed model of nonstationary self-action of a high-power laser radiation, accounting for the delay of the cubic susceptibility of the air medium, the

contribution from the material dispersion in the third-order approximation, and the contribution from nonlinearity of the gas plasma, whose generation is described by the Perelomov–Popov–Terent'ev photoionization theory with the experimental estimate of the effective charge, adequately describes generation of the conical emission of the supercontinuum. The frequency-angular dependence for the supercontinuum radiation derived from this model is quantitatively close to the experimental data.

3. Physically, generation of the conical emission of supercontinuum is explained by self-phase modulation of the light field in space and time that occurs at strong optical nonlinearity under the conditions of high space and time localization of radiation. The frequency-angular dependence of the conical emission of supercontinuum is determined by the dynamic field of nonlinear change of the light wave phase. This field is formed as a result of the joint effect of many factors in the nonlinear optical interaction of radiation with the air medium.

The models of generation of the conical emission of supercontinuum using the concept of self-trapping and involving the effects on the filament surface are inconsistent, because in the complex dynamic spatial distribution of the light field there is no long channel for propagation of the radiation.

4. The model developed and presented in this paper allows numerical simulation of a high-power femtosecond laser pulse propagation in air with different parameters of the initial radiation. In particular, it allows studying the effect of the initial phase modulation of the laser pulse and beam divergence on the process of generation of the conical emission of supercontinuum.

Acknowledgments

This work was partially supported by the Russian Foundation for Basic Research Grant No. 00–02–17497.

References

1. S.A. Akhmanov, V.A. Vysloukh, and A.S. Chirkin, *Optics of Femtosecond Laser Pulses* (Nauka, Moscow, 1988), 310 pp.
2. V.P. Kandidov, O.G. Kosareva, A. Broder, and S.L. Chin, Atmos. Oceanic Opt. **10**, No. 12, 966–973 (1997).
3. A. Braun, G. Korn, X. Lin, D. Du, J. Squier, and G. Mourou, Opt. Lett. **20**, 73 (1995).
4. E.T.J. Nibbering, P.F. Curley, G. Grillon, B.S. Prade, M.A. Franco, F. Salin, and A. Mysyrowicz, Opt. Lett. **21**, 62–64 (1996).
5. A. Brodeur, O.G. Kosareva, C.Y. Chien, F.A. Ilkov, V.P. Kandidov, and S.L. Chin, Opt. Lett. **22**, 304–306 (1997).
6. O.G. Kosareva, V.P. Kandidov, A. Brodeur, and S.L. Chin, Nonlinear Opt. Phys. & Mat. **6**, 485–494 (1997).
7. B.L. Fontaine, F. Vidal, Z. Jiang, C.Y. Chein, D. Corntois, A. Desparois, T.W. Jonston, J.-C. Kieffer, H. Pepin, and H.P. Mercure, Physics of Plasmas **6**, No. 3, 1815 (1999).
8. S. Tzortzakis, B. Lamouroux, A. Chiron, M. Franco, B. Prade, A. Mysyrowicz, and S.D. Moustaizis, Opt. Lett. **25**, No. 17, 1270–1272 (2000).
9. O.G. Kosareva, V.P. Kandidov, A. Brodeur, C.Y. Chien, and S.L. Chin, Opt. Lett. **22**, No. 17, 1332–1334 (1997).
10. L. Woste, C. Wedekind, H. Wille, P. Rairoux, B. Stein, S. Nikolov, Chr. Werner, St. Niedermaier, F. Ronnerberger, H. Schillinger, and R. Sauerbrey, Laser and Optoelectronik **29**, No. 5 51–54 (1997).
11. L. Woste, C. Wedekind, H. Wille, P. Rairoux, M. Rogriguez, B. Stein, R. Sauerbrey, H. Schillinger, F. Ronnerberger, and St. Niedermaier, in: *Ultrafast Phenomena XI. Proc of the 11th Intern. Conf.*, Garmisch-Partenkirchen, Germany, July 12–17, 1998, pp. 118–119.
12. J. Kasparian, R. Sauerbrey, D. Mondelian, S. Niedermeier, J. Yu, J.-P. Wolf, Y.-B. Andre, M. Franco, B. Prade, S. Tzortzakis, A. Mysyrowicz, M. Rodriguez, H. Wille, and L. Woste, Opt. Lett. **25**, No. 18, 1397–1399 (2000).
13. V.M. Gordienko, A.I. Kholodnykh, and V.I. Pryalkin, Kvant. Elektron. **30**, No. 9, 839–842 (2000).
14. M.E. Genshaw and C.D. Cantrell, Phys. Rev. A **39**, 126–148 (1989).
15. V.B. Morozov, A.N. Olenin, and V.G. Tunkin, Kvant. Elektron. **25**, No. 4, 293–294 (1998).
16. H.R. Lange, G. Grillon, J.-F. Ripoche, M.A. Franko, B. Lamouroux, B.S. Prade, and A. Mysyrowicz, Opt. Lett. **23**, No. 2, 120–122 (1998).
17. Q. Xing, K.M. Yoo, and R.R. Alfano, Appl. Opt. **32**, 2087–2089 (1993).
18. G.G. Luther, A.C. Newell, J.V. Moloney, and E.M. Wright, Opt. Lett. **19**, No. 11, 789–791 (1994).
19. I. Golub, Opt. Lett. **15**, No. 6, 305–307 (1990).
20. E. Baubean, F. Salin, and C. Le Blanc, in: *Ultrafast Phenomena XI. Proc of the 11th Intern. Conf.*, Garmisch-Partenkirchen, Germany, July 12–17, 1998, pp. 81–83.
21. S.C. Rae, Opt. Commun. **104**, 330–335 (1994).
22. M.L. Ter-Mikaelian, G.A. Torossian, and G.G. Grigoryan, Opt. Commun. **119**, 56–60 (1995).
23. S.L. Chin, A. Brodeur, S. Petit, O.G. Kosareva, and V.P. Kandidov, J. Nonlinear Opt. Phys. Mater. **8**, 121–146 (1999).
24. I.S. Golubtsov, O.G. Kosareva, and E.I. Mozhaev, Physics of Vibrations **8**, No. 2, 73–78 (2000).
25. A.M. Perelomov, M.V. Popov, and M.V. Terent'ev, Zh. Eksp. Teor. Fiz. **50**, No. 5, 1393–1410 (1966).
26. A. Talebpour, *"Semi-empirical model for the rate of tunnel ionization of* N_2 *and* O_2 *molecule in an intense* Ti*:sapphire laser pulse,"* Ph. D. Thesis (Laval, 1998).
27. P.A. Oleinikov and V.T. Platonenko, Laser Physics **3**, No. 3, 618–622 (1993).
28. E.T.J. Nibbering, G. Grillon, M.A. Franco, B.S. Prade, and A. Mysyrowicz, J. Opt. Soc. Am. B **14**, No. 3, 650–660 (1997).
29. V.E. Zuev, A.A. Zemlyanov, and Yu.D. Kopytin, *Nonlinear Optics of the Atmosphere* (Gidrometeoizdat, Leningrad, 1989), 256 pp.
30. D.V. Vlasov, R.A. Garaev, V.V. Korobkin, and R.V. Serov, Zh. Eksp. Teor. Fiz. **76**, No. 6, 2039–2045 (1979).
31. Y. Shimoji, A.T. Fay, R.S.F. Chang, and N. Djeu, J. Opt. Soc. Am. B **6**, No. 9, 1994–1998 (1989).
32. M. Mlejnek, E.M. Wright, and J.V. Moloney, Opt. Lett. **23**, No. 5, 382–384 (1998).
33. O.G. Kosareva, *"Propagation of high-power subpicosecond laser pulse in gases under ionization conditions,"* Cand. Phys.-Math. Sci. Dissert. (Moscow, 1995), 137 pp.
34. V.P. Kandidov, O.G. Kosareva, E.I. Mozhaev, and M.P. Tamarov, Atmos. Oceanic Opt. **13**, No. 5, 394–401 (2000).
35. *Handbook of Chemistry and Physics* (CRC Press, 1984–1985).
36. S.L. Chin, N. Akozbek, A. Proulx, S. Petit, and C.M. Bowden, Opt. Commun. **188**, 181–186 (2001).